Analytical Methods

Accepted Manuscript

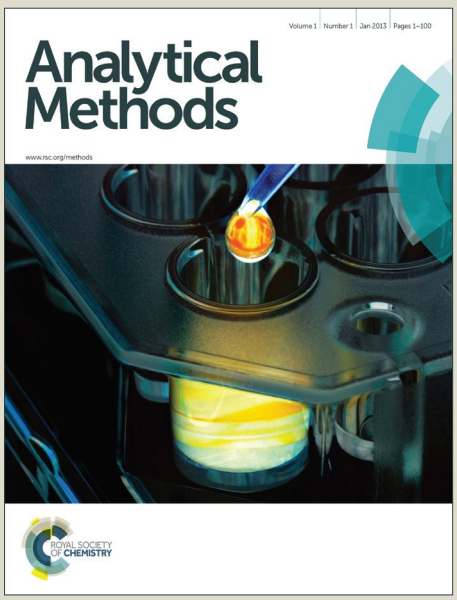

This is an *Accepted Manuscript*, which has been through the Royal Society of Chemistry peer review process and has been accepted for publication.

Accepted Manuscripts are published online shortly after acceptance, before technical editing, formatting and proof reading. Using this free service, authors can make their results available to the community, in citable form, before we publish the edited article. We will replace this *Accepted Manuscript* with the edited and formatted *Advance Article* as soon as it is available.

You can find more information about *Accepted Manuscripts* in the Information for Authors.

Please note that technical editing may introduce minor changes to the text and/or graphics, which may alter content. The journal's standard Terms & Conditions and the Ethical guidelines still apply. In no event shall the Royal Society of Chemistry be held responsible for any errors or omissions in this *Accepted Manuscript* or any consequences arising from the use of any information it contains.

ROYAL SOCIETY OF CHEMISTRY

www.rsc.org/methods

ARTICLE TYPE www.rsc.org/xxxxxx | XXXXXXXX

Well-Defined Sulfamethazine-Imprinted Magnetic Nanoparticles *via* Surface-Initiated Atom Transfer Radical Polymerization for Highly Selective Enrichment of Sulfonamides in Food Samples

Xuedong Mao[a,b], Hongyu Sun[a,b], Xiwen He[a,b],Langxing Chen[a,b,*], Yukui Zhang[a,b,c]

Received (in XXX, XXX) Xth XXXXXXXXX 200X, Accepted Xth XXXXXXXXX 200X
First published on the web Xth XXXXXXXXX 200X
DOI: 10.1039/b000000x

In this work, a novel kind of core-shell magnetic molecularly imprinted polymers (MIP) for sulfamethazine (SMZ) was synthesized by surface-initiated atom transfer radical polymerization (ATRP) strategy. In this protocol, the polydopamine was formed on the Fe_3O_4 nanoparticles (NPs) in 10 mM Tris-HCl buffer solution (pH 8.5). The initiator bromide reagent of ATRP was then grafted onto the polydopamine surface. Finally, the MIP layer was formed on the surface of Fe_3O_4 by the copolymerization of sulfamethazine as template, methacrylic acid as functional monomer, ethylene glycol dimethacrylate as cross-linking agent using organometallic catalyst comprising Cu(I)Br and pentamethyldiethylenetriamine. The morphology, magnetic, adsorption and recognition properties of Fe_3O_4@SMZ-MIP NPs were characterized using transmission electron microscope (TEM), Fourier transform infrared (FT-IR) spectrometer, vibrating sample magnetometer (VSM), X-ray diffractometer (XRD), thermogravimetric analysis (TGA) and re-binding experiments. The controllable nature of ATRP allows the growth of uniform MIP layer with adjustable thickness, providing a large adsorption capacity (680.27 μg g^{-1}), a fast kinetics about 40 min to equilibrium, and a considerable high imprinting factor with 17.02. The feasibility of enrichment of sulfonamides by Fe_3O_4@SMZ-MIP was demonstrated using egg samples spiked with SMZ and SMR. The recoveries of SMZ and SMR ranged from 76.7 to 93.0% and 69.3 to 77.2%, respectively and the relative standard deviations (RSD) (< 7.0%). In addition, Fe_3O_4@SMZ-MIP showed good reusability for at least five repeated cycles.

1. Introduction

The sulfonamides (SA) are a family of synthetic broadspectrum antibiotic drugs used in veterinary clinical treatment and in animal feeds to promote livestock growth[1,2]. The continual over use of sulfonamides can lead to the antibacterial resistance, and then do harm to human health and ecological environment[3,4]. Because of the safety concern, licensed uses of sulfonamides is now limited. The European Commission (EC), America and other countries, for example China, have adopted a maximum acceptable limit of residual sulfonamide in foods of animal origin, for example meat, milk and eggs in order to control illegal usage and exceeding contamination that would affect human health[5]. Therefore, there is an urgent need to establish a reliable, rapid, sensitive and low cost method for monitoring the trace levels of sulfonamide residues in foods, environmental and biological samples. Several methods have been reported for detecting sulfonamides in the numerous matrices[6], such as high-performance liquid chromatography (HPLC)[7,8] and gas chromatography (GC)[9,10], high-performance liquid chromatography–mass spectrometry (HPLC–MS)[11], HPLC/MS/MS[12] and capillary electrophoresis (CE) [13]. Due to the interference from the complex matrix, sample preparation is a key step prior to the detection of sulfonamides present in various matrices. Many sample preparation methods, including liquid-liquid extraction (LLE)[14], solid-phase extraction (SPE)[15] and solid phase microextraction (SPME)[16,17] have been applied for extraction of sulfonamides. To improve the efficiency and selectivity by which analytes are isolated, the application of SPE/SPME procedure involving the use of molecularly imprinted polymers (MIPs), a novel type of adsorbent, called MISPE, has been widely applied for preconcentration and separation of trace analytes in the complex samples[18-22].

MIPs are tailor-made materials that can exhibit high affinity and selectivity towards a given target or group of target molecules, which are prepared by copolymerization of functional monomers and cross-linkers around a template. Extraction of the template leaves behind recognition sites of functional and shape complementarity to the template[23,24]. Unlike antibodies, enzymes or biological receptors, MIPs possess the greater stability and applicability in harsh chemical media without loss of binding properties, as well as lower cost, rapid and easier preparation. Several MIPs for sulfonamides[25-37] have been prepared as the stationary phase

[a]*State Key Laboratory of Medical Chemical Biology, Research Center for Analytical Science, College of Chemistry, Nankai University, Tianjin 300071, P.R. China. Fax: 86 22 23502458; E-mail: lxchen@nankai.edu.cn*
[b]*Collaborative Innovation Center of Chemical Science and Engineering (Tianjin)*
[c]*Dalian Institute of Chemical Physics, Chinese Academy of Sciences, Dalian 116023, P. R. China. E-mail: ykzhang@dicp.ac.cn*

for HPLC and as solid-phase extracting agents in the past decade. However, most MIPs for sulfonamides have been synthesized in bulk polymerization, followed by a grinding and sieving process to acquire the desired particles, which suffer from several disadvantages, including heterogeneous distribution of the binding sites, poor site accessibility, and low mass transfer. To resolve these disadvantages, a surface imprinting has been proposed as a feasible strategy for sulfonamides imprinting[38-40]. In the previous study, we developed the synthesis of silica-coated MIPs nanospheres for selective extraction of sulfonamides from milk and eggs samples with highly imprinting effect and adsorption capacity[28]. The magnetic nanoparticles coated with MIPs will facilitate the recognition and can be easily isolated from the real samples. We also reported the core-shell magnetic MIPs prepared by copolymerization of vinyl grafted to the surface of Fe_3O_4 and functional monomer methacrylic acid (MAA), and applied magnetic MIPs to separate and enrich sulfamethazine from the poultry feed samples[35]. Dai et al. synthesized a 13 nm MIP shell through reverse atom transfer radical polymerization (RAFT), which exhibited excellent selectivity and good reuse in the analysis of sulfamethazine[41]. There is an increasing MIPs which have been prepared via controlled/living radical polymerization[42]. The atom transfer radical polymerization (ATRP)[43,44], a catalyst-activated controllable radical polymerization method produces no solution phase radical species, the solution-phase polymerization is avoided. Because ATRP can provide definite structure and uniform molecular weight distribution, it has been used to graft MIPs from solid substrate[45-50].

In this work, we develop a surface-initiated ATRP strategy for highly dense imprinting of sulfamethazine (SMZ) at the surface of Fe_3O_4 NPs. The sulfamethazine-imprinted Fe_3O_4 (Fe_3O_4@SMZ-MIP) NPs possess good biocompatible properties, and could be easily isolated from samples by using an external magnetic field without the need of complicated centrifugation steps or filtration. Moreover, it exhibited the greater imprinting factor and quick mass transfer in the sulfamethazine adsorption. Importantly, it worked well when it was applied to the enrichment of sulfamethazine and sulfamerazine in spiked eggs.

2. Experimental

2.1 Chemicals

The five sulfonamides including sulfamethazine (SMZ), sulfadiazine (SDZ), sulfamerazine (SMR), sulfameter (SME) and sulfamethoxazole (SMO) were obtained from Sigma–Aldrich (USA), and their structures are shown in Figure 1. The methacrylic acid (MAA), ethyleneglycol dimethacrylate (EGDMA), 2-bromoisobutyrylbromide and 1,1',4,7,7'-pentamethyldiethylenetriamine (PMDETA) were also purchased from Sigma–Aldrich (USA). Dopamine and 4-dimethylaminopyridine (DMAP) were purchased from Alfa Aesar. Azo-bis-isobutyronitrile (AIBN) was provided by Shanghai Chemicals. $FeCl_3$•$6H_2O$, CuBr, ammonium acetate, sodium citrate, methanol, ethanol, acetonitrile, hydrochloric acid, acetic acid, phosphoric acid, dichloromethane and triethylamine were purchased from Tianjin Chemicals (China). HPLC-grade acetonitrile (ACN) was purchased from Merck (Darmstadt, Germany). All reagents used were of analytical or HPLC grade and used without further purification. Highly purified water (18MΩ cm^{-1}) obtained from a WaterPro Water System (Aquapro Corporation, AFZ-6000-U, China) was used in the experiments. analyses. Highly purified water was prepared with a Milli-Q water purification system (Millipore, Milford, MA).

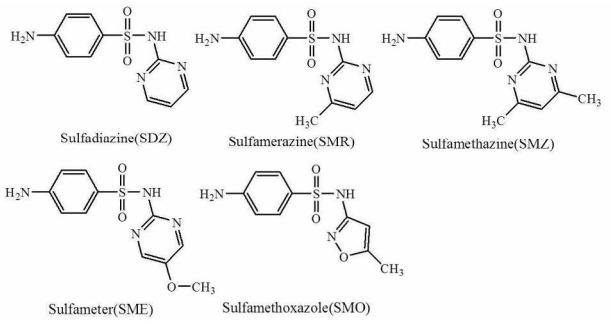

Figure 1 Molecular structure of the five sulfonamides (SMZ, SDZ, SMR, SME and SMO) used in this study.

2.2 Characterization

The morphology of Fe_3O_4, polydopamine-coated Fe_3O_4 (Fe_3O_4@PDA) and Fe_3O_4@SMZ-MIP NPs were examined by Tecnai G2 T2 S-TWIN TEM. The infrared spectra of Fe_3O_4, Fe_3O_4@PDA, Fe_3O_4@PDA-Br and Fe_3O_4@SMZ-MIP were recorded with Nicolet AVATAR-360 FT-IR spectrometer. After vacuum drying, the magnetic particle samples were thoroughly mixed with KBr (weight ratio of sample/KBr was 1%) in a mortar, and then pressed the fine power into a pellet. Then the FT-IR spectrum was recorded. The magnetic properties were analyzed with a vibrating sample magnetometer (VSM) (LDJ 9600-1, USA). The identification of the crystalline phase of obtained Fe_3O_4, Fe_3O_4@PDA, Fe_3O_4@PDA-Br and Fe_3O_4@SMZ-MIP NPs was performed on a Rigaku D/max/2500v/pc(Japan) X-ray diffractometer with a Cu Kasource. The 2θ angles sprobed were from 10° to 80° at a rate of 4° min^{-1}. Thermogravimetric analysis (TGA) was performed in nitrogen atmosphere at a heating rate of 10°C min^{-1} from room temperature to 800℃ (NETZSCH, TG209, Germany).

2.3 HPLC analysis

The HPLC analyses were performed on a Shimadzu LC-20A HPLC system including a variable wavelength UV detector (Shimadzu, Kyoto, Japan). The instrument control and data processing were carried out by the LC solution software. A Shimadzu VP-ODS C18 (5 μm particle size, 150 mm × 4.6 mm) analytical column was used for analytes separation. The mobile phase was acetonitrile-10 mmol L^{-1} H_3PO_4 (0-13 min (12:88, v/v), 13-30 min (12:88-30:70, v/v), 30-50 min (30:70-12:88, v/v)) at a flow rate of 1.0 mL min^{-1}. The injection volume was 20 μL, and the column effluent was monitored at 270 nm.

2.4 Preparation of core-shell sulfamethazine-imprinted Fe_3O_4 particles (Fe_3O_4@SMZ-MIP)

First, Fe_3O_4 nanoparticles (NPs) were synthesized according to a solvothermal method as reported previously[51]. Typically, 0.675g $FeCl_3$•$6H_2O$, 1.925 g NH_4Ac and 0.2 g sodium citrate were dissolved in 35 mL ethylene glycol and then transferred in a Teflon-lined stainless-steel autoclave, sealed and heated to 200°C for 16 h. After the autoclave was cooled to room temperature, the obtained Fe_3O_4 NPs were washed 5 times with water and ethanol, and collected using a magnet, and then dried under vacuum at 50°C.

The Fe_3O_4 NPs was then modified with dopamine to introduce amine groups[52]. Briefly, 100 mg Fe_3O_4 NPs were dispersed in 50 mL 10 mM Tris-HCl (pH 8.5) buffer solution by 15 min sonication. Next 50 mg dopamine was added the mixture, and the reaction solution was mechanically stirred at 500 rpm for 12h. The product defined as Fe_3O_4@polydopamine (Fe_3O_4@PDA) was separated by a magnet, washed with highly purified water 5 times, and dried under vacuum at 50°C.

The detail of the synthesis of Fe_3O_4@initiator was as the following[50]. 300 mg Fe_3O_4@PDA, 30 mL dichloromethane, 1 mL triethylamine, and 1.3 mg DMAP as a catalyst were added individually into around flask, followed with 15 min sonication. The mixture was bubbled with high-purity nitrogen at 0°C for half an hour. Then 300 µL 2-bromoisobutyrylbromide was added, and the mixture was mechanically stirred at room temperature for 12 hours. The product Fe_3O_4@PDA@Br was washed with dichloromethane 5 times, and finally dried at room temperature.

The SMZ surface-imprinted polymers were synthesized by ATRP procedure[49]. Firstly, 0.2226 g SMZ (0.8 mmol) as template, 0.407 ml MAA (4.8 mmol) as monomer, 4 ml EGDMA (24mmol) as cross linking agent were dissolved in 12 mL acetonitrile for prepolymerization at room temperature. Then, transferred the mixture to a three-neck round-bottom flask, and added 120 mg Fe_3O_4@PDA@Br. The mixture was mechanically stirred at 300 rpm till it was well-distributed. After the air was exchanged with nitrogen three times, 25 µL PMDETA and 11.2 mg CuBr were quickly added. With freeze-pump-thaw three times, the system proceeded at 70°C with mechanical stirring for 24h. The polymer was washed with acetonitrile and water several times to remove any unreacted substances and then immersed into CH_3OH-HAc (v/v, 9:1) to remove the templates. Finally, the product Fe_3O_4@SMZ-MIP was dried under vacuum at 50°C. Correspondingly, without template imprinted polymers (Fe_3O_4@NIP) was generated in the same way without adding SMZ.

2.5 Adsorption properties studies of Fe_3O_4@SMZ-MIP and Fe_3O_4@NIP

In kinetic adsorption experiment, 10 mg Fe_3O_4@SMZ-MIP were suspended in 3 mL 40 µg mL^{-1} SMZ acetonitrile solutions, and incubated at regular time intervals, and then the supernatants were separated by the magnet. The concentration of SMZ in the supernatants was measured by HPLC analysis.

In thermodynamic adsorption experiment, 10 mg Fe_3O_4@SMZ-MIP and Fe_3O_4@NIP were suspended in 3 mL SMZ acetonitrile solutions of various concentrations from 0.1 to 60 µg mL^{-1}, and shook for 40 min. The concentration of SMZ in the supernatants of Fe_3O_4@SMZ-MIP and Fe_3O_4@NIP was measured by HPLC analysis.

In selective adsorption experiment, 10 mg Fe_3O_4@SMZ-MIP and Fe_3O_4@NIP were suspended in 3 mL 40 µg mL^{-1} mixed acetonitrile solution of SMZ and its analogues (SDZ, SMR, SME, SMO), and then shook for 40 min. The concentration of five analytes in the supernatants of Fe_3O_4@SMZ-MIP and Fe_3O_4@NIP was measured by HPLC analysis.

2.6 Reusability of Fe_3O_4@SMZ-MIP

To estimate the reusability of Fe_3O_4@SMZ-MIP, 10 mg polymers were added to the solutions of SMZ in 3 mL 40 µg mL^{-1} SMZ and shook for 40 min. Then, Fe_3O_4@SMZ-MIP were separated by the magnet and the bound amount of SMZ was measured by HPLC. The recovered Fe_3O_4@SMZ-MIP were washed with CH_3OH-HAc (v/v, 9:1) till we ensure complete removal of residual SMZ in the polymers and washed with ethanol for several times, then dried under vacuum at 50◦C and reused for adsorption of SMZ.

2.7 Separation and determination of SMZ and SMR in eggs

Eggs purchased from the market were spiked with SMZ and SMR at three concentration levels: 0.1, 0.2 and 0.5 µg g^{-1}. First, 20 mL ethanol-water (v/v, 6:4) was added to 4 g egg sample spiked the standard SMZ and SMR mixed solution in a 50 mL polypropylene tube. The mixed sample was shaken for 2 h, then centrifuged at 3000 rpm for 10 min, the supernatant solution was filtered through a 0.22 µm filter[28]. The filtrate was dried by rotary evaporator, and then dissolved in 50 mL acetonitrile. Next, 20 mg Fe_3O_4@SMZ-MIP was added to 10 mL of the above treated solution and then incubated for 40 min. After discarding the supernatant solution using a magnet, the polymer which had absorbed the target molecule was eluted with 9:1 (v/v) methanol–acetic acid. Finally, the eluent was collected and dried by rotary evaporator, and then the residue was dissolved in 1 mL acetonitrile and measured by HPLC.

3. Result and Discussion

3.1 Preparation and characterization of Fe_3O_4@SMZ-MIP

The synthesis of Fe_3O_4@SMZ-MIP via a multistep procedure is illustrated in Figure 2. Firstly, the polydopamine (PDA) layer formed on the surface of Fe_3O_4 NPs in a weak alkaline Tris-HCl buffer solution (pH 8.5). Recently, catecholic amino acid 3,4-dihydroxy-L-phenylalanine secreted from mussels binds strong to a broad spectrum of inorganic and organic surfaces[52]. It has been reported that dopamine was utilized as a versatile and intriguing started material for solid surface modification and autopolymerized to form PDA films under mild condition[52-55]. The PDA coating on magnetic Fe_3O_4 remain stable even if in harsh environment such as strong acid solution, so it can protect the magnetic particles from etching in acid solution. The conjugation to PDA is easily adapted for

a variety of materials without surface pretreatment, and more important, it offers selectivity of reaction with amine or imidazole functional groups of a variety of molecules. The secondary amino groups of PDA could be easily modified with 2-bromoisobutyrylbromide to introduce the initiator. Then, initiator bromide reagent was efficiently grafted onto the PDA surface. Finally, MIP shell was coated onto the surface of Fe_3O_4@PDA@Br NPs via ATRP, after extraction of templates to generate the recognition sites.

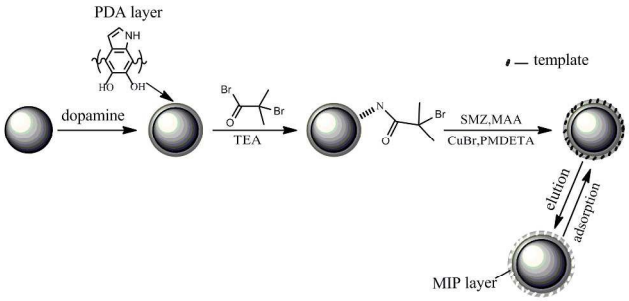

Figure 2 Outline of the fixation of an ATRP agent onto Fe_3O_4 NPs and the grafting of MIP shell from Fe_3O_4 NPs via ATRP.

TEM images of Fe_3O_4, Fe_3O_4@PDA, and Fe_3O_4@SMZ-MIP were shown in Figure 3. The Fe_3O_4 NPs were regular spherical particles with a mean diameter of about 300 nm (Figure 3a). After coating with dopamine, the PDA layer with a thickness of 20 nm existed on the surface of Fe_3O_4 NPs (Figure 3b). The TEM image of Fe_3O_4@SMZ-MIP displayed the shell further increase along with imprinting process. It is estimated that the diameter of the resulting MIP layer was about 15 nm (Figure 3c). The value was basically consistent with the previous work[49,50]. The uniform and thin layer was expected to be effective to the mass transport between solution and the surface of Fe_3O_4@SMZ-MIP.

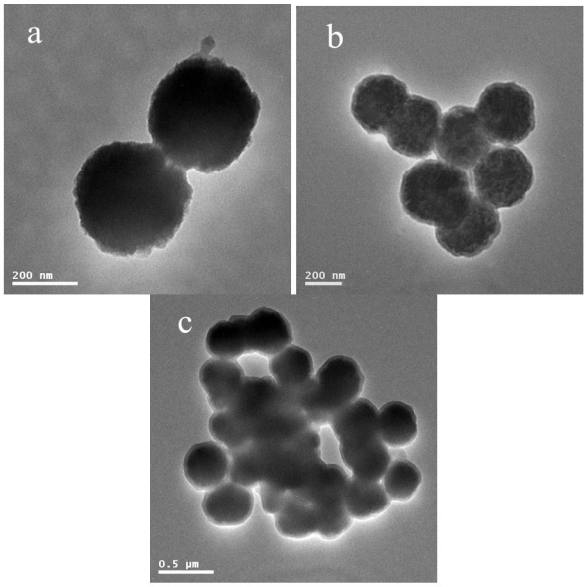

Figure 3 TEM images of (a) Fe_3O_4, (b)Fe_3O_4@PDA, and (c) Fe_3O_4@SMZ-MIP particles.

The FT-IR spectra of Fe_3O_4, Fe_3O_4@PDA, Fe_3O_4@PDA-Br, Fe_3O_4@SMZ-MIP and Fe_3O_4@NIP were compared in Figure 4. The bands of 1595 cm^{-1} and 1406 cm^{-1} (Figure 4a) are corresponding to the stretching vibrations of asymmetric COO- and symmetric COO- on the Fe_3O_4 NPs using citrate as stable agent. The bands from 1500 to 1641 cm^{-1} (Figure 4b) can be attributed to the characteristic peaks of phenyl group, and the new peak at 2980 cm^{-1} is -NH-. The notable change from Figure 4b to Figure 4c is the disappearance of 2980 cm^{-1} peak, which demonstrates the initiator had been modified to Fe_3O_4@PDA. The peaks of 2920 and 1438 cm^{-1} represent C-H of methyl and C-O respectively, which demonstrates the imprinted polymer coatings had been successfully grafted from Fe_3O_4@ PDA-Br. The absorption bands of Fe_3O_4@NIP prepared without SMZ is almost the same as Fe_3O_4@SMZ-MIP which obtained after removal of SMZ (Figure 4e).

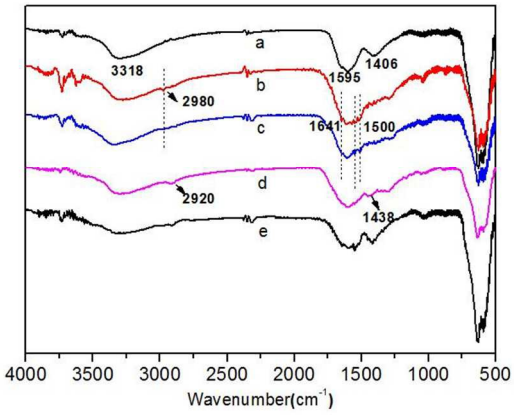

Figure 4 FT-IR spectra of (a) Fe_3O_4, (b) Fe_3O_4@PDA, (c) Fe_3O_4@PDA-Br, (d) Fe_3O_4@SMZ-MIP and (e) Fe_3O_4@NIP particles.

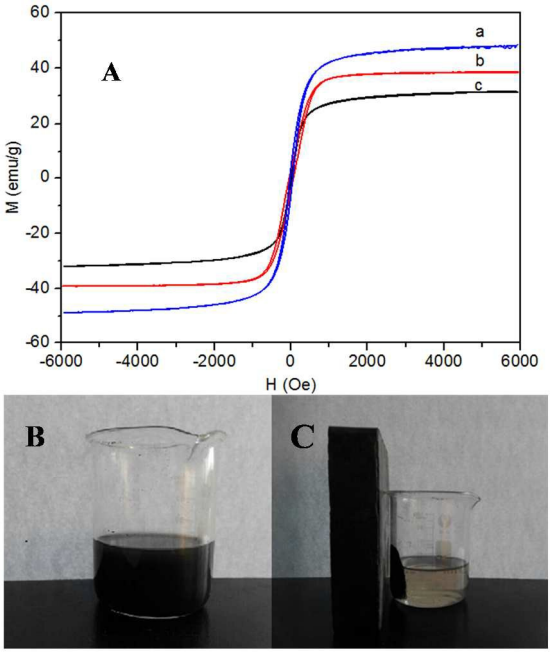

Figure 5 (A) Magnetization curve of Fe_3O_4 (a), Fe_3O_4@PDA-Br (b) and Fe_3O_4@SMZ-MIP (c); (B) dispersion of Fe_3O_4@SMZ-MIP; (C) separation of Fe_3O_4@SMZ-MIP by a magnet.

Vibrating sample magnetometry (VSM) was employed to study the magnetic properties of the synthesized magnetic nanoparticles. The magnetic hysteresis loops of the dried samples at room temperature were illustrated in Figure 5A. It is obvious that there is no hysteresis, both remanence and coercivity are zero, suggesting that the samples are superparamagnetism. The saturation magnetization values were 48.56, 38.18 and 31.85 emu g^{-1} for Fe_3O_4, Fe_3O_4@PDA-Br and Fe_3O_4@SMZ-MIP, respectively. Compared with Fe_3O_4, the decrease in magnetization value of Fe_3O_4@PDA-Br and Fe_3O_4@SMZ-MIP is attributed to the PDA layer and imprinted shell on the surface of Fe_3O_4 NPs to influence the magnetic response of Fe_3O_4 NPs. However, the magnetic Fe_3O_4@SMZ-MIP NPs still performed strongly magnetic strength at room temperature and allowed for effective magnetic separation. Figure 5B, 5C showed the dispersion and separation process of Fe_3O_4@SMZ-MIP. In the absence of an external magnetic field, a dark homogeneous dispersion existed. When a magnet was applied, the black particles were attracted to the wall of the beaker and the dispersion became clear and transparent.

The crystalline structure of synthesized Fe_3O_4, Fe_3O_4@PDA-Br and Fe_3O_4@SMZ-MIP were determined by powder X-ray diffraction (XRD) (Figure 6). In the 2θ range of 20–80°, six characteristic peaks for Fe_3O_4 (2θ = 30.38°, 35.58°, 43.14°, 53.48°, 57.08° and 62.66°) were observed for the three samples. The peaks at the corresponding 2θ values were indexed as (220), (311), (400), (422), (511), and (440) respectively, which matched well with the database for magnetite in the JCPDS-International Center for Diffraction Data (JCPDS Card: 19-629) file. The XRD patterns also show that PDA, Br atoms and MIP functionalization on MNPs did not change the Fe_3O_4 phase.

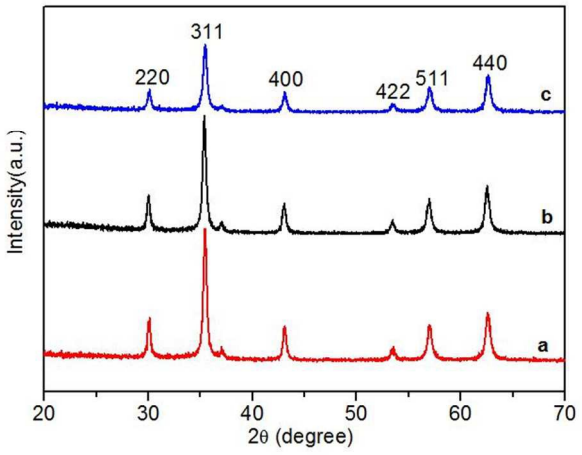

Figure 6 XRD patterns of Fe_3O_4 (a), Fe_3O_4@PDA-Br (b) and Fe_3O_4@SMZ-MIP (c).

TGA was employed to further estimate grafting yield of polymer coating and quantify the amount of Fe_3O_4 encapsulated in the magnetic particles. As shown in Figure 7a, about 17.5% weight loss is observed on the curve of cirtate stabilized Fe_3O_4 NPs corresponding to the evaporation of the adsorbed solvent and the decomposition of citrate. In Figure 7b, a more 10% weight loss is due to decomposition of organic structure of the PDA layer. As shown in Figure 7b and Figure 7c, there exsits 15.81% weight difference between Fe_3O_4@PDA-Br and Fe_3O_4@SMZ-MIP related to the MIP layer, which means the imprinted shell content was roughly 15.81 wt% and the remaining magnetite content is around 56.72 wt% in Fe_3O_4@SMZ-MIP.

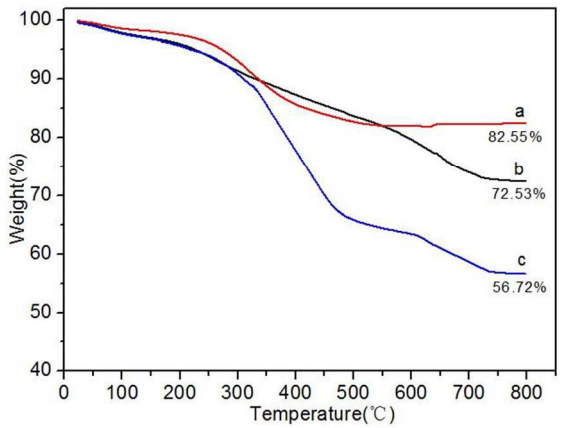

Figure 7 TGA curves of of Fe_3O_4 (a), Fe_3O_4@PDA-Br (b) and Fe_3O_4@SMZ-MIP (c).

3.2 The binding capacity and kinetic study of imprinted materials

The binding capacity and kinetic study of the imprinted core-shell materials Fe_3O_4@SMZ-MIP prepared by the ATRP strategy were investigated. Figure 8A presents the adsorption kinetics of SMZ solution onto Fe_3O_4@SMZ-MIP. It is required only about 40 min to reach equilibrium for SMZ, making it be a time-saving method to apply for the practical analysis. The result justly demonstrated that the uniform and thin layer could make the imprinted sites more accessible and effective to the mass transport, thus overcame some drawbacks of traditionally packed imprinted materials.

Further studies were carried out to determine the binding isotherms of SMZ onto Fe_3O_4@SMZ-MIP and Fe_3O_4@NIP in the concentration range of 0.1-60 μg mL^{-1} (initial concentration) and the results were shown in Figure 8B. It is obvious that the amount of SMZ bound to the Fe_3O_4@SMZ-MIP increased quickly along with the increasing initial concentration of SMZ when it was below 40 μg mL^{-1}. In contrast, the amount of SMZ bound to NIP was a low and nearly steady level. The adsorption curve reaches saturation at a high concentration of 40 μg mL^{-1}.

To gain further insight into the phenomenon of SMZ binding by the Fe_3O_4@SMZ-MIP nanoparticles, the binding data were fitted into a Langmuir isotherm model. The Langmuir equation is as follows:

$$[SMZ]/Q=1/(Q_{max}\ K_D)+[SMZ]/Q_{max}$$

Where Q is the amount of SMZ bound to Fe_3O_4@SMZ-MIP at equilibrium, Q_{max} is the apparent maximum adsorption capacity, [SMZ] is the free analytical concentration at equilibrium and K_D is the dissociation constant. The values of

K_D and the Q_{max} can be calculated from the slope and intercept of the above equation.

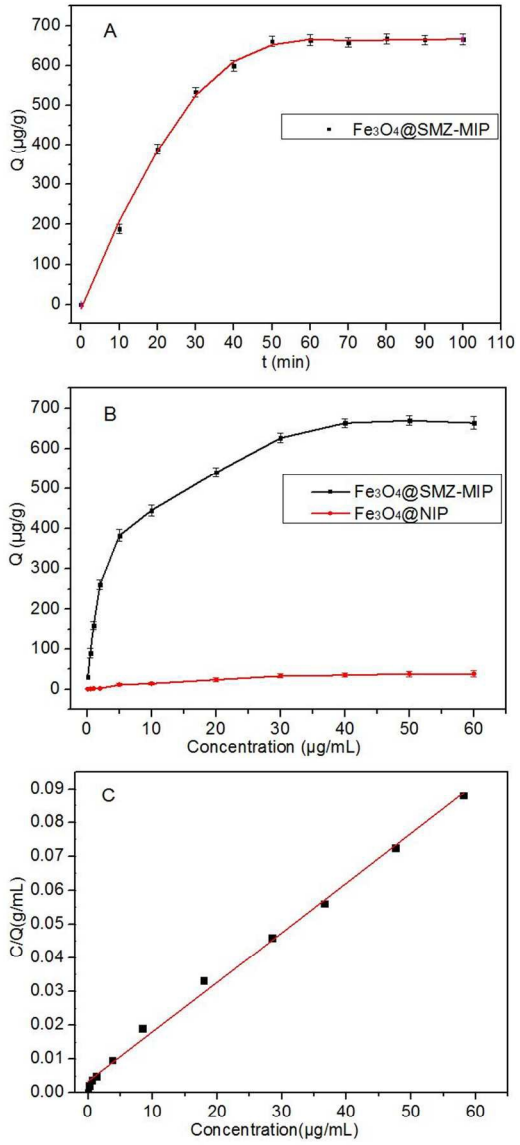

Figure 8 (A) Adsorption kinetics of Fe_3O_4@SMZ-MIP to SMZ. Condition: 10 mg Fe_3O_4@SMZ-MIP NPs dispersed in 3 mL 40 μg mL^{-1} SMZ solutions. (B) Adsorption isotherms of Fe_3O_4@SMZ-MIP and Fe_3O_4@NIP to SMZ. Condition: 10 mg MIP or NIP dispersed in 3 mL 0.1-60 μg mL^{-1} SMZ solutions. (C) Langmuir plot to estimate the binding mechanism of Fe_3O_4@SMZ-MIP towards SMZ.

According to Langmuir model, adsorption was occurred uniformly on the active sites of the adsorbent. Once a template molecule occupied the site, no further adsorption could take place at this site. It was observed that the experimental data was fitted to Langmuir adsorption isotherm model in Figure 8C. The adsorption process of SMZ onto Fe_3O_4@SMZ-MIP could be considered the monolayer adsorption. The linear regression equation for the linear region is [SMZ]/Q=0.00342+0.00147[SMZ] (r=0.9979). From the slope and the intercept of the straight line obtained, the values of K_D and Q_{max} were 0.420 mL μg^{-1} and 680.27 $\mu g\ g^{-1}$ respectively.

3.3 The specific selectivity of SMZ imprinted materials

In order to verify the specific selectivity of the Fe_3O_4@SMZ-MIP to the template SMZ, four other sulfonamide analogs SDZ, SMR, SME and SMO (Figure 1) were selected as the comparative substrates. As shown in Figure 9, we can see that the amount of SMZ bound to MIP decreased to 321.97 $\mu g\ g^{-1}$ in comparison with only SMZ in solution. On the contrary, the amount of SDZ and SMR bound to MIP had a relatively high level of 98.71 and 90.86 $\mu g\ g^{-1}$, and only the amount of SMO was very low about 26.98 $\mu g\ g^{-1}$. The results are ascribed to SMZ, SDZ, SMR and SME possess the closer structure, which have two N atoms in the pyrimidine ring, whereas SMO has one N atom and one O atom in the oxazole ring. Because the specific sites existed in the imprinted polymers are complementary in shape, size and spatial distribution to template molecule, the template molecule has advantage in occupying the binding sites over the other sulfonamides, Fe_3O_4@SMZ-MIP showed the highest binding capacity. And because the structure of five sulfonamides is analogous, the binding capacity of Fe_3O_4@SMZ-MIP to SMZ, SMO, SME, SMR and SDZ is greater than that of Fe_3O_4@NIP.

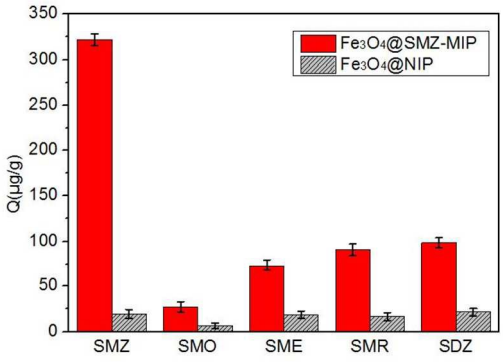

Figure 9 Binding capacity of Fe_3O_4@SMZ-MIP and Fe_3O_4@NIP towards five sulfonamides in the mixture in which SMZ, SMO, SME, SMR and SDZ with a concentration of 40 $\mu g\ mL^{-1}$ for each compound.

Additionally, the partition coefficients, the imprinting factor (IF) and selectivity coefficient (SC) were used to evaluate the imprinting effect and selectivity properties of MIP and NIP toward template and other competitors. The partition coefficient K was determined according to the following formula[56]:

$$K=C_p/C_s$$

Where C_p is the amount of test analyte bound by Fe_3O_4@SMZ-MIP or Fe_3O_4@NIP and C_s is the concentration of test analyte remaining in solution.

IF is taken as the ratio of partition coefficient of analyte for the Fe_3O_4@SMZ-MIP and Fe_3O_4@NIP and SC is defined as the ratio of IF of template with respect to that of other

competitor. The IF for binding SMZ was 17.02, and is also higher than that of the other surface imprinting technology for sulfonamides[28, 33-35]. The IF of other sulfonamides SMR, SDZ, SME and SMO were 5.51, 4.62, 3.97 and 4.08, respectively (Table 1). The results further demonstrated that the excellent imprinting efficiency of the present ATRP method and Fe_3O_4@SMZ-MIP was expected to be applied to the enrichment of sulfonamides.

Table 1 The adsorption capacity, partition coefficients, imprinting factors and selectivity coefficients of SMZ and its analogues SMO, SME, SMR and SDZ for the imprinted Fe_3O_4@SMZ-MIP and control Fe_3O_4@NIP NPs[a] (n=3).

Analytes	Q_{MIPs} (μg g^{-1})	Q_{NIPs} (μg g^{-1})	K_{MIPs} (mL g^{-1})	K_{NIPs} (mL g^{-1})	IF	SC
SMZ	321.97	19.31	8.14	0.48	17.02	–
SMO	26.98	6.63	0.68	0.17	4.08	4.18
SME	73.57	18.59	1.84	0.46	3.97	4.29
SMR	90.86	16.57	2.29	0.41	5.51	3.09
SDZ	98.71	21.46	2.48	0.54	4.62	3.68

[a]In this experiment, 10 mg of Fe_3O_4@SMZ-MIP or Fe_3O_4@NIP NPs, were added to the 3 mL of acetonitrile solution containing the mixture of SMZ, SMO, SME, SMR and SDZ with a concentration of 40 μg mL^{-1} for each compound.

3.4 Reusability of SMZ imprinted materials

To examine the reusability of MIP, adsorption–desorption cycle was repeated five times by using the same Fe_3O_4@SMZ-MIP. The adsorbed SMZ could be eluted with CH_3OH-HAc (v/v, 9:1). In Figure 10, there is about 10.2% loss was observed for the binding capacity of Fe_3O_4@SMZ-MIP to SMZ after 5 cycles. The loss may be caused by the blockage and the destruction of some recognition sites in the network of Fe_3O_4@SMZ-MIP during several cycles. The results indicated that the Fe_3O_4@SMZ-MIP particles can be reused at least 5 times, which is a clear advantage over single-use materials.

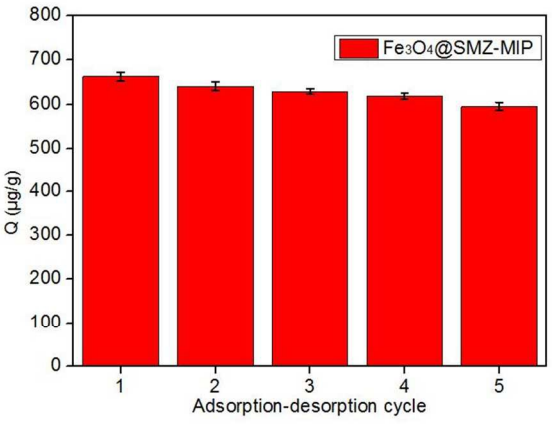

Figure 10 Reusability of Fe_3O_4@SMZ-MIP.

3.5 Application of Fe_3O_4@SMZ-MIP in the enrichment of SMZ and SMR in egg samples

The applicability of Fe_3O_4@SMZ-MIP in the enrichment of SMZ and SMR in egg samples was demonstrated. The chromatograms of spiked SMR and SMZ at a concentration of 0.1 μg g^{-1} before adsorption and the elution of adsorbed Fe_3O_4@SMZ-MIP to SMR and SMZ washed with a mixing methanol-HAc (9:1, v/v) after adsorbing egg samples are displayed in Figure 11. As presented in the chromatograms, when the spiked level was 0.1 mg/kg, there is no peaks for SMR and SMZ without enrichment step. After the enrichment, the peaks of SMR and SMZ appeared distinctly at 8.2 min and 11.6 min, respectively. The chromatograms confirmed that the Fe_3O_4@SMZ-MIP could be applied to the enrichment of SMR and SMZ in egg samples.

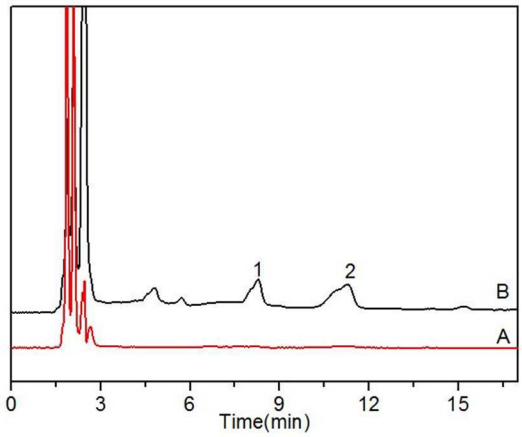

Figure 11 Chromatograms of SMR (1) and SMZ (2) in spiked eggs. (A) Samples spiked with SMZ at the concentration of 1 mg kg^{-1} before adsorption (A) and the elution of Fe_3O_4@SMZ-MIP washed with a mixture of methanol/HAc (9:1, v/v) after Fe_3O_4@SMZ-MIP adsorbing the spiked samples.

The calibration curve ranging from 0.050 to 20 μg mL^{-1} with the highly linear regression coefficients ($r > 0.9998$) by injecting of 20 μL standard solution was obtained for SMR and SMZ. The detection limit which was calculated as the concentration corresponding to a signal-to-noise ratio of three was 11.62 and 14.36 μg L^{-1} for SMR and SMZ, respectively.

To evaluate the accuracy and application of the developed method, eggs spiked with three levels (0.1, 0.2, and 0.5 μg g^{-1}) of SMR and SMZ were analyzed. Table 2 lists the recoveries and relative standard deviation (RSD) of SMR and SMZ, expressed as the mean value (n =5). The recovery of SMZ ranged from 76.7 to 93.0%, while the SMR from 69.3 to 77.2%. The recoveries of SMZ and SMR of less than 80% are similar to the recoveries of four tetracycline antibiotics,[57] β_2-agonists spiked feed samples,[58] which are roughly equivalent to our recent work,[28,35] the recoveries of SDZ in milk samples and SMZ in the poultry feed samples. The RSD were less than 7.0%. These results revealed that the Fe_3O_4@SMZ-MIP can be directly used for selective adsorption and determination of SMR and SMZ in food samples.

Table 2 Recoveries of SMR and SMZ in the spiked eggs with 0.1, 0.2, and 0.5 mg kg^{-1} after using Fe_3O_4@SMZ-MIP as adsorbent (n=5).

Analytes in eggs samples	0.1 mg kg^{-1}		0.2 mg kg^{-1}		0.5mg kg^{-1}	
	Recovery (%)	RSD (%)	Recovery (%)	RSD (%)	Recovery (%)	RSD (%)
SMR	69.3	7.0	72.9	4.8	77.2	4.0
SMZ	76.7	4.2	87.1	3.7	93.0	3.0

4. Conclusion

In summary, we developed a novel strategy combining MIT and ATRP for preparation of core-shell magnetic MIP as adsorbent in the enrichment of SMZ and SMR in egg samples. Although, the ATRP method is extremely sensitive to the oxygen requiring strict operation and needs metal catalyst which will do harm to certain template, but the results in the work demonstrated that the controllable nature of ATRP allows the growth of uniform MIP layer with adjustable thickness, providing a considerable high imprinting factor (IF=17.02), a fast kinetics with only 40 min to reach adsorption equilibrium and high binding capacity (Q_{max}=680.27 μg g^{-1}) and can be easily isolated from the real samples by using a magnet. Successful application in the selective separation and enrichment of SMR and SMZ from egg samples and good recovery after a reasonably mild elution suggested that the functional MIPs coated magnetic NPs could be an alternative solution for selective enrichment of antibiotic residuals in a complex matrix like environmental, food, feed and biological samples. Moreover, the ATRP route can be potential to used in the preparation of various MIP for other templates like biomacromolecules with various solid support (such as quantum dots, gold nanoparticles and carbon nanotubes).

Acknowledgements

The authors are grateful to the National Basic Research Program of China (No. 2012CB910601), the National Natural Science Foundation of China (No. 21275080, 21475067), Research Fund for the Doctoral Program of Higher Education of China (No. 20120031110007) and the National Natural Science Foundation of Tianjin (No. 15JCYBJC20600).

References

1 C. Cháfer-Pericás, Á. Maquieira, R. Puchades, Trends Anal. Chem., 2010, **29**, 1038-1049.
2 M. R. Payán, M. A. B. López, R. Fernández-Torres, M. V. Navarro, M. C. Mochón, J. Chromatogr. B, 2011, **879**, 197-204.
3 A. M. Bueno, A. M. Contento, Á. Rios, J. Sep. Sci., 2014, **37**, 382-389.
4 S. O'Connor, D. S. Aga, Trends Anal. Chem., 2007, **26**, 456-465.
5 N. Furusawa, Anal. Chim. Acta, 2003, **481**, 255.
6 S. G. Dmitrienko, E. V. Kochuk, V. V. Apyari, V. V. Tolmacheva, Y. A. Zolotov, Anal. Chim. Acta, 2014, **850**, 6-25.
7 A. Preechaworapun, S. Chuanuwatanakul, Y. Einaga, K. Grudpan, S. Motomizu, O. Chailapakul, Talanta, 2006, **68**, 1726.
8 E. P. Tolika, V. F. Samanidou, I. N. Papadoyannis, Curr. Pharm. Anal., 2010, **6**, 198-212.
9 B. Chiavarino, M.E. Crestoni, A.D. Marzio, S. Fornarini, J. Chromatogr. B,1998, **706**, 269.
10 V.B. Reeves, J. Chromatogr. B, 1999, **723**, 127.
11 S. Bogialli, R. Curini, A.D. Corcia, M. Nazzari, R. Samperi, Anal. Chem., 2003, **75**, 1798.
12 S. Borràs, R. Companyó, J. Guiteras, J. Bosch, M. Medina, S. Termes, Anal. Bioanal. Chem., 2013, **405**, 8475-8486.
13 R. Hoff, T. B. L. Kist, J. Sep. Sci., 2009, **32**, 854-866.
14 J. Chico, A. Rúbies, F. Centrich, R. Companyó, M. Prat, M. Granados, J. Chromatogr. A, 2008, **1213**, 189–199.
15 J. Raich-Montiu, J. Folch, R. Compañó, M. Granados, M. D. Prat, J. Chromatogr. A, 2007, **1172**, 186–193.
16 B. Shao, D. Dong, Y. N. Wu, J. Y. Hu, J. Meng, X. M. Tu, S. K. Xu, Anal. Chim. Acta, 2005, **546**, 174–181.
17 Y. Hu, J. Pan, K. Zhang, H. Lian, G. Li, Trends Anal. Chem., 2013, **43**, 37-52.
18 C. Baggiani, L. Anfossi, C. Giovannoli, Anal. Chim. Acta, 2007, **591**, 29.
19 F. Puoci, M. Curcio, G. Cirillo, F. Iemma, U.G. Spizzirri, N. Picci, Food Chem., 2008, **106**, 836.
20 F.G. Tamayo, E. Turiel, A. Martín-Esteban. J. Chromatogr. A, 2007, **1152**, 32.
21 X.L. Sun, X.W. He, Y.K. Zhang, L.X. Chen, Talanta, 2009, **79**, 926.
22 R. Schirhagl, Anal. Chem., 2014, **86**, 250-261.
23 M. Yan, O. Ramström, Molecularly Imprinted Materials: Science and Technology, Marcel Dekker, New York, 2005.
24 L. Chen, S. Xu, J. Li, Chem. Soc. Rev., 2011, **40**, 2922–2942.
25 N. Zheng, Y.Z. Li, M.J. Wen, J. Chromatogr. A, 2004, **1033**, 179.
26 X.J. Liu, C.B. Ouyang, R. Zhao, D.H. Shangguan, Y. Chen, G.Q. Liu, Anal. Chim. Acta, 2006, **571**, 235.
27 M. Valtchev, B.S. Palm, M. Schiller, U. Steinfeld, J. Hazard. Mater., 2009, **170**, 722.
28 R.X. Gao, J.J. Zhang, X.W. He, L.X. Chen, Y.K. Zhang, Anal. Bioanal. Chem., 2010, **398**, 451.
29 L.G. Chen, X.P. Zhang, L. Sun, Y. Xu, Q.L. Zeng, H. Wang, H.Y. Xu, A. Yu, H.Q. Zhang, L. Ding, J. Agric. Food Chem., 2009, **57**, 10073.
30 Z.Y. Chen, R. Zhao, D.H. Shangguan, G.Q. Liu, Biomed. Chromatogr., 2005, **19**, 533.
31 M.P. Davies, V.D. Biasi, D. Perrett, Anal. Chim. Acta, 2004, **504**, 7.
32 A. Guzmán-Vázquez de Prada, P. Martínez-Ruiz, A.J. Reviejo, J.M. Pingarrón, Anal. Chim. Acta, 2005, **539**, 125.
33 J.X. He, S. Wang, G.Z. Fang, H.P. Zhu, Y. Zhang, J. Agric. Food Chem., 2008, **56**, 2919.
34 S.F. Su, M. Zhang, B.L. Li, H.Y. Zhang, X.C. Dong, Talanta, 2008, **76**, 1141.
35 X. Kong, R.X. Gao, X.W. He, L.X. Chen, Y.K. Zhang, J. Chromatogr. A, 2012, **1245**, 8-16.
36 S. L. Qin, S. Deng, L. Q. Su, P. Wang, Anal. Methods, 2012, **4**, 4278-4283.
37 M. Díaz-Álvarez, F. Barahona, E. Turiel, A. Martín-Esteban, J. Chromatogr. A, 2014, **1357**, 158-164.
38 E. Yilmaz, K. Haupt, K. Mosbach, Angew. Chem. Int. Ed., 2000, **39**, 2115-2118.
39 A Bossi, S.A. Piletsky, E.V. Piletska, P.G. Righetti, A.P.F. Turner, Anal. Chem., 2001, **73**, 5281.
40 R.X. Gao, X.Q. Su, X.W. He, L.X. Chen, Y.K. Zhang, Talanta, 2011, **83**, 757.
41 J.D. Dai, Z.P. Zhou, Y.L. Zou, J. Appl. Polym. Sci., 2014, **131**, 40854.
42 H. Wang, X. Dong, M. Yang, Trends Anal. Chem., 2012, **31**, 96-108.
43 K. Matyjaszewski, T. E. Pattern, J. Xia, J. Am. Chem. Soc., 1997, **119**, 674.
44 K. Matyjaszewski, N.V. Tsarevsky, Nat. Chem., 2009, **1**, 276.
45 X.L. Wei, X. Li, S.M. Husson, Biomacromolecules, 2005, **6**, 1113-1121.
46 X.L. Wei, S.M. Husson, Ind. Eng. Chem. Res., 2007, **46**, 2117-2124.
47 H. Kong, C. Gao, D. Yan, J. Am. Chem. Soc., 2004, **126**, 412.
48 H. J. Wang, W. H. Zhou, X. F. Yin, Z. X. Zhuang, H. H. Yang, X. R. Wang, J. Am. Chem. Soc., 2006, **128**, 15954.
49 C.H. Lu, Y. Wang, Y. Li, H.H. Yang, X. Chen, X.R. Wang, J. Mater. Chem., 2009, **19**, 1077-1079.
50 Q.Q. Gai, F. Qu, Z.J. Liu, R.J. Dai, Y.K. Zhang, J. Chromatogr. A, 2010, **1217**, 5035-5042.
51 S.H. Xuan, Y. Xiang, J. Wang, J.C. Yu, K.C.F. Leung, Chem. Mater., 2009, **21**, 5079-5087.
52 H. Lee, S.M. Dellatore, W.M. Miller, P.B. Messersmith, Science, 2007, **318**, 426-430.
53 S.M. Kang, N.S. Hwang, J. Yeom, S.Y. Park, P.B. Messersmith, I.S. Choi, R. Langer, D.G. Anderson, H. Lee, Adv. Funct. Mater., 2012, **22**, 2949-2955.
54 M. Zhang, X.W. He, L.X. Chen, Y.K. Zhang, J. Mater. Chem., 2010, **20**, 10696-10704.
55 M. Zhang, X.H. Zhang, X.W. He, L.X. Chen, Y.K. Zhang, Nanoscale, 2012,**4**, 3141-4147.
56 J. Zhou, X.W. He, Anal. Chim. Acta, 1999, **381**, 85.
57 X.G. Hu, J.L. Pan, Y.L. Hu, Y. Huo, G.K. Li, J. Chromatogr. A, 2008, **1188**, 97-107.
58 Z.G. Xu, Y.F. Hu, Y.L.Hu, G.K. Li, J. Chromatogr. A, 2010, **1217**, 3612-3618.